Published in final edited form as:
Basic Res Cardiol. 2008 March ; 103(2): 122–130. doi:10.1007/s00395-008-0710-7.

Magnetic nanoparticles for MR imaging: agents, techniques and cardiovascular applications

David E. Sosnovik, MD, FACC[1,2], **Matthias Nahrendorf, MD**[1], and **Ralph Weissleder, MD, PhD**[1,3]

1 *Center for Molecular Imaging Research, Massachusetts General Hospital, 149 13th Street, Charlestown (MA) 02129, USA*

2 *Dept. of Cardiology, Massachusetts General Hospital, Harvard Medical School, Boston (MA), USA*

3 *Center for Systems Biology, Massachusetts General Hospital, Harvard Medical School, Boston (MA), USA*

Abstract

Magnetic nanoparticles (MNP) are playing an increasingly important role in cardiovascular molecular imaging. These agents are superparamagnetic and consist of a central core of iron-oxide surrounded by a carbohydrate or polymer coat. The size, physical properties and pharmacokinetics of MNP make them highly suited to cellular and molecular imaging of atherosclerotic plaque and myocardial injury. MNP have a sensitivity in the nanomolar range and can be detected with T1, T2, T2*, off resonance and steady state free precession sequences. Targeted imaging with MNP is being actively explored and can be achieved through either surface modification or through the attachment of an affinity ligand to the nanoparticle. First generation MNP are already in clinical use and second generation agents, with longer blood half lives, are likely to be approved for routine clinical use in the near future.

Keywords

molecular; imaging; MRI; nanoparticles; iron oxide; cardiovascular

Introduction

The advantages of an MRI-based approach to cardiovascular imaging include its high spatial resolution, excellent soft tissue contrast and ability to simultaneously image cardiovascular anatomy, physiology and molecular events [32]. The role of molecular MRI in cardiovascular medicine has been broadly examined in several recent reviews, and the interested reader is referred to these articles for a comprehensive discussion of the field [11,32]. In the current article, however, we focus specifically on the role of magnetic nanoparticles (MNP) in cardiovascular molecular imaging. In the initial portion of the article the physical characteristics of several generations of MNP are reviewed. The advantages and disadvantages of various strategies with which to image MNP are then discussed. Finally, the role of these agents in the diagnosis and study of cardiovascular disease is reviewed.

Tel.: +1-617/726-5788, Fax: +1-617/726-5708, E-Mail: sosnovik@nmr.mgh.harvard.edu.

Conflict of Interest Dr Weissleder is a shareholder of VisEn Medical in Woburn (MA), USA. The other authors report no conflicts.

Agents

The principal challenge of molecular MRI, in comparison to other molecular imaging techniques such as PET and fluorescence, lies in its lower sensitivity. Conventional gadolinium chelates have a sensitivity in the micromolar range which, with certain exceptions, is usually inadequate for molecular MRI. Conventional extracellular gadolinium chelates also have extremely short intravascular half-lives and rapid renal excretion, which further limits their utility for most molecular imaging applications.

Several novel gadolinium constructs have been developed to address these limitations and are discussed in more detail in other articles in this supplement. These constructs are heavily loaded with paramagnetic gadolinium chelates and in general have longitudinal relaxivity (R1) values ranging from 10 to 20 s^{-1} mM^{-1}[5,23]. The relaxivity of an MR contrast agent reflects its ability to interact with adjacent protons and strongly influences its detectability. The higher the longitudinal relaxivity (R1) of an agent, the brighter tissue in its vicinity becomes, while the higher the transverse relaxivity (R2), the darker the tissue becomes. Gadolinium based probes are generally imaged with T1 weighted sequences at standard clinical field strengths producing positive contrast. However, the R1 of these agents decreases rapidly at high field strengths reducing the sensitivity of these probes at high field.

MNP are typically superparamagnetic (but can also be synthesized to be ferromagnetic or paramagnetic, however these materials are not very useful for MR imaging) and can be imaged with T1, T2, T2* and steady state free precession techniques [7,19,33]. MNP agents typically have a central core of iron-oxide, measuring 3–5 nm in diameter, surrounded by a carbohydrate (for macrophage targeting) or polymer coat (often for targeting to other cells) [28,45]. A citrate coated iron-oxide nanoparticle has also recently been developed and used as a blood pool agent [39]. Selected MNP have been used extensively in the clinical arena to image the liver and lymphatic system [6], and their established safety record thus makes them a highly appealing platform for molecular MRI. A selected list of representative MNP is provided in Table 1. The R2 values of these agents range from 50 to >600 s^{-1} mM^{-1} [21,45], and remain constant over all field strengths >0.5 Tesla. The R1 values of these agents, however, decrease with field strength much like paramagnetic gadolinium constructs.

Several generations of MNP have now been synthesized, as shown in Fig. 1. The first generation of MNP, such as Feridex (Advanced Magnetics, Cambridge MA), contain relatively thin dextran coats and have the propensity to form polycrystalline clusters, which are rapidly cleared from the blood stream by the reticulo-enthothelial system. This agent can thus be used to detect the replacement of normal liver tissue by neoplasm and metastases, and has been FDA-approved for this application via intravenous injection since 1993. The metabolism, pharmacokinetics and toxicity of MNP taken up by cells in the reticulo-endothelial system have been well studied [42]. Histologic and serologic studies have not revealed any toxic effects related to MNP administration. Iron radiotracer (59FE) and MR relaxivity studies have also shown that the iron-oxide core of the MNP is broken down into other forms of iron and then incorporated normally into hemoglobin in newly formed erythrocytes [42]. More recently, several groups have used Feridex and other iron oxide nanoparticles to label exogenous stem cells prior to their in vivo administration [9,17]. The pharmacokinetics, metabolism and safety profile of Feridex when used for cell labeling, however, will require additional evaluation.

Subsequent generations of MNP (Fig. 1) have been synthesized with more extensive polymer coatings and remain monodisperse in solution [28]. The term monocrystalline iron oxide or MION is thus often applied to these agents. Unlike Feridex, these agents were designed to have a much longer blood half live (24 h in humans, 11 h in mice) and typically have a homogenous uniform size distribution in the 30–50 nm range [28,45,46]. The small size, long blood half

lives and high relaxivities of these MNP constitute a powerful combination that allows them to penetrate deep tissue spaces, such as the interior of atherosclerotic plaque and the myocardium [12,31], and detect sparsely expressed targets in the low nanomolar range. The MNP Ferumoxtran (Combidex or Sinerem), a preparation similar to the experimental MION-47, has been used to image lymph node micrometastases in several phase 3 clinical trials [6]. This agent has also been used to image inflamed vulnerable plaque in humans [16, 36], although the experience in this regard is preliminary and is discussed in the article by Nahrendorf and colleagues in this supplement.

A highly stabilized and cross-linked derivative of MION-47, known as CLIO-47, has also recently been developed for targeted molecular imaging applications [18,45]. CLIO contains amine groups on cross-linked dextran chains, allowing a large variety of ligands to be conjugated to the nanoparticle with a high degree of stability and relative ease. Near infrared fluorochromes, for instance, can be attached to the amine groups on the probe to form a dual modality magnetofluorescent nanoparticle [15,27]. In addition, many copies of the targeting ligand can subsequently be attached to the CLIO-fluorochrome conjugate to form a multivalent (>1 targeting ligand) magnetofluorescent nanoparticle. Examples of two recently used such ligands include annexin for apoptosis imaging [27,33], and a peptide specific for the adhesion molecule VCAM-1 [14,24]. More recently an experimental MNP with even higher relaxivity (MION-48, CLIO-48, R2 > 180 s^{-1} mM^{-1}) has been synthesized, and has the potential to enhance the sensitivity of these and other targeted probes even further.

Molecular MR agents can be targeted to a specific entity through one of two mechanisms. The first involves the attachment of an affinity ligand (antibody, fragments, proteins, peptides, apatamers) directed against a known target on the cell surface, such as the $\alpha_v\beta_3$ integrin [22, 43], phosphatidylserine [27,37], or VCAM-1 [14,24]. The second approach involves modification of the MNP surface with small molecules to modulate its uptake [35,40]. Although these small chemical moeties are several orders of magnitude smaller than the MNP, they have been shown to dramatically influence the target binding and in vivo kinetics of these probes through a variety of mechanisms. High-throughput screening of a library of surface-modified MNP, for instance, has revealed agents that are highly specific for either resting or activated macrophages [40]. This demonstrates that MNP may be targeted not only to cell type but also to cell state. In addition, it suggests that the uptake of MNP such as MION by macrophages is more complex than initially thought and not necessarily an automatic consequence of a macrophage encountering a synthetic nanoparticle. Coating an MNP with the small chemical SIA (succinimidyl iodo acetate), for instance, can dramatically reduce its uptake by both resting and activated macrophages [40].

The size and physical properties of certain MNP, such CLIO, also promote cellular internalization of the MNP after ligand binding to an appropriate receptor [10,14]. Once within the cell the MNP become trapped and compartmentalized within lysosomes producing strong biological amplification of the signal [10]. This amplification is due to an increase in R2 when a given concentration of MNP becomes compartmentalized or aggregated in cells rather than remaining disperse in solution [29]. This concept has been demonstrated by several groups and also forms the basis of the magnetic relaxation switches, developed in our laboratory, for bioassays [26].

Imaging techniques

The superparamagnetic nature of MNP allows T2* weighted imaging to be performed with equal accuracy at all field strengths above 0.5 T, at which the R2 and R2* of these agents plateau. As one moves to a higher field strength, however, a given amount of T2 or T2* weighting can be achieved at progressively shorter echo times because of an increase in the

transverse relaxation rates of the surrounding tissues with field. Moving to higher field thus not only increases the signal and contrast to noise ratios, but also reduces motion and flow artifacts by reducing the required echo time. T1 weighted imaging can also be robustly performed with MNP but must be done at standard clinical field strengths where their R1 values remain high, and also with echo times short enough to avoid R2 effects [19].

The sensitivity of MNP has been well documented with a variety of techniques, most notably T2* weighted and SSFP imaging [7,24,33]. In an environment where the diffusion of water is completely unrestricted the sensitivity of T2 weighted imaging will approach that of T2* weighted imaging. In most scenarios involving cardiovascular imaging with MNP, however, diffusion in the vessel wall or myocardium is significantly restricted and a T2* weighted approach is more sensitive. SSFP imaging has been used in a clinical system fitted with high performing animal gradients to image even single cells loaded with MNP in the brain [8]. Tissue contrast in SSFP is a combination of T2 and T1 effects and is highly non linear, being heavily influenced by amongst other factors the echo spacing in the sequence. For instance, when the resonance offset angle of the steady state magnetization approaches ±180° an abrupt and dramatic local loss of signal occurs. This phenomenon can be exploited to detect MNP but may also produce off-resonance artifacts in areas with no MION, particularly at higher fields. Further study will be needed with SSFP sequences in areas other than the brain and with applications other than stem cell imaging to better define the role of this technique.

When either T2, T2* or SSFP sequences are used the presence of the MNP is imaged through the generation of negative contrast or relative signal hypointensity. Concerns have been raised that this negative contrast could be non-specific and difficult to discern from signal hypointensity due to calcification, susceptibility artifacts, flow related signal loss or air (Table 2). In addition, particularly in the area of stem cell imaging the linearity of T2* based imaging as a function of cell number or MNP content has been questioned. Several off-resonance techniques have thus been developed to generate positive contrast from MNP and potentially address these concerns [3,20,34].

Positive contrast techniques include those that selectively excite off-resonance spins [3], exploit saturation transfer from the off-resonance to the on-resonance proton pool, modulate the slice rephasing gradient to fully rephase only those spins that experience additional rephasing from the dipole field generated by the MNP [20], and sequences that suppress on-resonance protons with either inversion recovery or chemical saturation techniques [4,34]. While the use of these positive contrast techniques will require further study, several recent reports provide initial insights into their diagnostic accuracy.

The sensitivity of the positive contrast sequences for MNP may approach that of conventional T2* based techniques, (nanomolar) [4,20], if performed under optimal conditions and with parameters producing low specificity. However, unlike conventional T2* techniques where the sensitivity for MNP at a given echo time increases with field strength, the converse holds true for the off-resonance techniques [4,20]. At higher fields the on-resonance water linewidth is broader producing a decrease in the spectral separation of on and off-resonance spins. Another challenge with these techniques, and at high field in particular, appears to be a nonlinear response to MNP concentration [4]. As the MNP content in a voxel increases, the percentage of spins shifted off resonance increases but the T2 of these shifted spins also becomes extremely short, opposing the positive contrast. The linearity of the positive contrast techniques particularly at high field strengths can thus become unpredictable, particularly if the echo time is not kept extremely short.

The average resonance shift induced by susceptibility artifacts at an air interface has recently been shown to be approximately 300 Hz at 4.7 Tesla, which corresponds to the shift obtained

with 150 ug Fe/ml of MION [4]. The imaging of MNP with positive contrast techniques in regions of the body with complex air interfaces is thus complicated by this non-specific shift, particularly at high field strengths where the shift is larger. Positive contrast techniques are thus likely to work best when high local concentrations of MNP are imaged at 1.5–3 Tesla. At these field strengths the on-resonance linewidth is narrowest and the non-specific off-resonance shifts are lowest [4]. This approach, for instance, has recently been shown by Stuber and colleagues to generate extremely high quality off-resonance angiograms of the rabbit aorta in vivo at 3 Tesla [34].

Newer gadolinium chelates have been used, to date, principally to image endothelial and other targets in atherosclerotic plaque such as macrophages [1], fibrin [2], and angiogenesis [44]. The imaging of these agents is usually performed with a T1 weighted sequence at standard field strengths, where the R1 of the probe remains high producing positive contrast. As with positive contrast techniques for MNP, however, several important artifacts need to be considered when using gadolinium based probes (Table 2). Fat has a high R1 value and appears bright on T1 weighted sequences. Incomplete suppression of the perivascular fat, for instance, can thus mimic uptake of the probe in the vessel wall. Slow flow within the vessel lumen can also result in incomplete suppression of the blood signal and thus mimic uptake of the probe within the endothelium [30]. Finally B1 inhomogeneity becomes a significant problem at higher fields and can produce significant variation in signal intensity due to inconsistent flip angles [38]. This B1 inhomogeneity will need to be addressed with techniques such as RF or B1 shimming, which requires multiple transmission coils and channels, if T1 weighted sequences are to be used optimally in humans and large animals at field strengths >3 Tesla [38].

A strong awareness of the sensitivity, specificity and artifacts produced by each imaging technique (T1, T2*, off-resonance) is thus needed (Table2). Methods to recognize and potentially eliminate some of these possible artifacts are provided in parentheses within Table 2. In extreme cases multi-modality imaging may be needed. However, one of the strengths of MRI lies in its ability to generate multiple forms of contrast, which can usually be used to differentiate any potential artifacts from a true molecular signal.

Cardiovascular applications

MNP have been used to image molecular targets in atherosclerosis [12,24], myocardial injury [25,31,33], and stem cell therapy [9,17]. The use of MNP in vascular imaging will be reviewed in the article by Nahrendorf and colleagues, and the role of these agents in stem cell imaging will be reviewed in the article by Kraitchman. The discussion below will thus focus purely on the imaging of myocardial injury with MNP.

The properties of MNP make them ideal agents with which to image myocardial macrophage infiltration in healing infarcts, transplant rejection and myocarditis [13,25,31]. This was recently demonstrated in a mouse model of post-infarction macrophage infiltration. The mice were injected intravenously with 3–20 mg Fe/kg of the MNP, CLIO-Cy5.5, 48 h after the infarct and then imaged with conventional T2* weighted MRI a further 48 h later. Negative contrast, consistent with the uptake of the probe by infiltrating macrophages, was seen in the infarcted anterolateral myocardium of all mice and at all doses [31], as shown in Fig. 2. It should be noted that the FDA approved dose for intravenous injections of clinically used MNP is 3 mg Fe/kg, and the ability of this experimental MNP to be detected at a dose of 3 mg Fe/kg is thus highly encouraging.

The T2* weighted MR images in Fig. 2a demonstrate another important finding. When contrast to noise was measured between the infarcted anterolateral and normal septal myocardium, a clear and fairly linear dose response to the MNP could be seen over a dose range up to seven

times higher than the clinically approved dose [31]. The images acquired in Fig. 2a were obtained with an echo time of 6.5 ms and thus the MNP produced marked signal hypointensity. However, as shown in Fig. 2b, shorter echo times could be used to reduce the T2* weighting and eliminate the signal hypointensity even in a mouse injected with 20 mg Fe/kg of the MNP [31]. The use of short echo times, T1 weighted or off-resonance positive contrast techniques can thus all be used to confirm that the negative contrast is not due to an artifact such as calcification (Table 2).

Targeted imaging of cardiomyocyte injury has been performed using two distinct MNP probes. Cardiomyocyte apoptosis has been imaged in vivo by MRI in a mouse model of transient coronary ligation [33]. No significant changes were seen in myocardial signal intensity when mice were injected with an unlabeled control probe. However, as shown in Fig. 3, injection of an identical dose (2 mg Fe/kg) of the annexin-labeled probe (AnxCLIO-Cy5.5) produced significant negative contrast enhancement in the injured myocardium [33]. T2* maps of the hypokinetic regions of the myocardium also showed significant differences in those mice given the active versus unlabeled probe, and the results were confirmed by fluorescence reflectance imaging of the near infrared fluorochrome on the probe [33]. Cardiomyocyte necrosis has also been imaged by MRI in the rat heart ex-vivo with an antimyosin antibody conjugated to MION [41]. The use of this probe in conjunction with apoptosis detecting probes could thus provide powerful insights into the pathogenesis of cell death during acute myocardial injury.

The myocardium is highly suited to multimodal molecular imaging approaches. Fluorescence tomography of the myocardium, for instance, has recently been performed in the mouse heart in vivo [25,31], as shown in Fig. 4. This is a completely non-invasive technique that is easily performed in conjunction with MRI of magnetofluorescent MNP and can be used in small animals, if necessary, to confirm the specificity of the changes in the MRI signal. In the large animal and human setting MRI of MNP can be combined with PET imaging either sequentially or simultaneously using novel MR-PET systems.

Conclusion and future outlook

MNP enhanced MRI of the cardiovascular system has been a fairly recent endeavor but these agents have already been used to image macrophage infiltration, apoptosis and VCAM-1 expression in small animal models in vivo. The sensitivity of targeted MNP is currently in the nanomolar range and will likely be improved through the use of agents with dramatically higher relaxivities than present constructs, and through optimization of pharmacokinetics using library approaches. The ability to image MNP with T1, T2, T2*, SSFP and off-resonance techniques provides multiple readouts to ensure probe specificity. Future MNP will further enhance specificity by allowing multi-modality imaging (MRI, fluorescence, PET) of the contrast agent to be performed. First generation polymer-coated MNP are currently FDA approved for clinical use and subsequent generations of MNP (Combidex, Advanced Magnetics, Cambridge MA) have already completed phase 3 clinical trials [6]. MRI of MNP in the cardiovascular system thus has the potential to become a powerful technology in both the basic science as well as the clinical settings.

Acknowledgements

Portions of this work have been supported by following National Institutes of Health grants: U01HL080731, R01HL07864, R01EB004626, P01CA117969-015904, R24-CA92782, K08 HL079984 (DES), and by the Donald W. Reynolds Cardiovascular Clinical Research Center, Harvard Medical School. Disclosures: RW is a shareholder of VisEN Medical in Woburn, MA.

References

1. Amirbekian V, Lipinski MJ, Briley-Saebo KC, Amirbekian S, Aguinaldo JG, Weinreb DB, Vucic E, Frias JC, Hyafil F, Mani V, Fisher EA, Fayad ZA. Detecting and assessing macrophages in vivo to evaluate atherosclerosis noninvasively using molecular MRI. Proc Natl Acad Sci USA 2007;104:961–966. [PubMed: 17215360]
2. Botnar RM, Perez AS, Witte S, Wiethoff AJ, Laredo J, Hamilton J, Quist W, Parsons EC Jr, Vaidya A, Kolodziej A, Barrett JA, Graham PB, Weisskoff RM, Manning WJ, Johnstone MT. In vivo molecular imaging of acute and subacute thrombosis using a fibrin-binding magnetic resonance imaging contrast agent. Circulation 2004;109:2023–2029. [PubMed: 15066940]
3. Cunningham CH, Arai T, Yang PC, McConnell MV, Pauly JM, Conolly SM. Positive contrast magnetic resonance imaging of cells labeled with magnetic nanoparticles. Magn Reson Med 2005;53:999–1005. [PubMed: 15844142]
4. Farrar C, Dai G, Rosen B, Sosnovik D. Off resonance imaging of superparamagnetic iron oxide nanoparticles in infarcted mouse myocardium at dilute concentrations and high magnetic field strengths. J Cardiovasc Magn Reson 2007;9:444–445.
5. Frias JC, Ma Y, Williams KJ, Fayad ZA, Fisher EA. Properties of a versatile nanoparticle platform contrast agent to image and characterize atherosclerotic plaques by magnetic resonance imaging. Nano Lett 2006;6:2220–2224. [PubMed: 17034087]
6. Harisinghani MG, Barentsz J, Hahn PF, Deserno WM, Tabatabaei S, van de Kaa CH, de la Rosette J, Weissleder R. Noninvasive detection of clinically occult lymph-node metastases in prostate cancer. N Engl J Med 2003;348:2491–2499. [PubMed: 12815134]
7. Heyn C, Bowen CV, Rutt BK, Foster PJ. Detection threshold of single SPIO-labeled cells with FIESTA. Magn Reson Med 2005;53:312–320. [PubMed: 15678551]
8. Heyn C, Ronald JA, Ramadan SS, Snir JA, Barry AM, Mackenzie LT, Mikulis DJ, Palmieri D, Bronder JL, Steeg PS, Yoneda T, Macdonald IC, Chambers AF, Rutt BK, Foster PJ. In vivo MRI of cancer cell fate at the single-cell level in a mouse model of breast cancer metastasis to the brain. Magn Reson Med 2006;56:1001–1010. [PubMed: 17029229]
9. Hill JM, Dick AJ, Raman VK, Thompson RB, Yu ZX, Hinds KA, Pessanha BS, Guttman MA, Varney TR, Martin BJ, Dunbar CE, McVeigh ER, Lederman RJ. Serial cardiac magnetic resonance imaging of injected mesenchymal stem cells. Circulation 2003;108:1009–1014. [PubMed: 12912822]
10. Hogemann-Savellano D, Bos E, Blondet C, Sato F, Abe T, Josephson L, Weissleder R, Gaudet J, Sgroi D, Peters PJ, Basilion JP. The transferrin receptor: a potential molecular imaging marker for human cancer. Neoplasia 2003;5:495–506. [PubMed: 14965443]
11. Jaffer FA, Libby P, Weissleder R. Molecular and cellular imaging of atherosclerosis: emerging applications. J Am Coll Cardiol 2006;47:1328–1338. [PubMed: 16580517]
12. Jaffer FA, Nahrendorf M, Sosnovik D, Kelly KA, Aikawa E, Weissleder R. Cellular imaging of inflammation in atherosclerosis using magnetofluorescent nanomaterials. Mol Imaging 2006;5:85–92. [PubMed: 16954022]
13. Kanno S, Wu YJ, Lee PC, Dodd SJ, Williams M, Griffith BP, Ho C. Macrophage accumulation associated with rat cardiac allograft rejection detected by magnetic resonance imaging with ultrasmall superparamagnetic iron oxide particles. Circulation 2001;104:934–938. [PubMed: 11514382]
14. Kelly KA, Nahrendorf M, Yu AM, Reynolds F, Weissleder R. In vivo phage display selection yields atherosclerotic plaque targeted peptides for imaging. Mol Imaging Biol 2006;8:201–207. [PubMed: 16791746]
15. Kircher MF, Mahmood U, King RS, Weissleder R, Josephson L. A multimodal nanoparticle for preoperative magnetic resonance imaging and intraoperative optical brain tumor delineation. Cancer Res 2003;63:8122–8125. [PubMed: 14678964]
16. Kooi ME, Cappendijk VC, Cleutjens KB, Kessels AG, Kitslaar PJ, Borgers M, Frederik PM, Daemen MJ, van Engelshoven JM. Accumulation of ultrasmall superparamagnetic particles of iron oxide in human atherosclerotic plaques can be detected by in vivo magnetic resonance imaging. Circulation 2003;107:2453–2458. [PubMed: 12719280]

17. Kraitchman DL, Heldman AW, Atalar E, Amado LC, Martin BJ, Pittenger MF, Hare JM, Bulte JW. In vivo magnetic resonance imaging of mesenchymal stem cells in myocardial infarction. Circulation 2003;107:2290–2293. [PubMed: 12732608]

18. Lewin M, Carlesso N, Tung CH, Tang XW, Cory D, Scadden DT, Weissleder R. Tat peptide-derivatized magnetic nanoparticles allow in vivo tracking and recovery of progenitor cells. Nat Biotechnol 2000;18:410–414. [PubMed: 10748521]

19. Li W, Salanitri J, Tutton S, Dunkle EE, Schneider JR, Caprini JA, Pierchala LN, Jacobs PM, Edelman RR. Lower extremity deep venous thrombosis: evaluation with ferumoxytol-enhanced MR imaging and dual-contrast mechanism–preliminary experience. Radiology 2007;242:873–881. [PubMed: 17325072]

20. Mani V, Briley-Saebo KC, Itskovich VV, Samber DD, Fayad ZA. Gradient echo acquisition for superparamagnetic particles with positive contrast (GRASP): sequence characterization in membrane and glass superparamagnetic iron oxide phantoms at 1.5T and 3T. Magn Reson Med 2006;55:126–135. [PubMed: 16342148]

21. Moffat BA, Reddy GR, McConville P, Hall DE, Chenevert TL, Kopelman RR, Philbert M, Weissleder R, Rehemtulla A, Ross BD. A novel polyacrylamide magnetic nanoparticle contrast agent for molecular imaging using MRI. Mol Imaging 2003;2:324–332. [PubMed: 14717331]

22. Montet X, Montet-Abou K, Reynolds F, Weissleder R, Josephson L. Nanoparticle imaging of integrins on tumor cells. Neoplasia 2006;8:214–222. [PubMed: 16611415]

23. Morawski AM, Winter PM, Crowder KC, Caruthers SD, Fuhrhop RW, Scott MJ, Robertson JD, Abendschein DR, Lanza GM, Wickline SA. Targeted nanoparticles for quantitative imaging of sparse molecular epitopes with MRI. Magn Reson Med 2004;51:480–486. [PubMed: 15004788]

24. Nahrendorf M, Jaffer FA, Kelly KA, Sosnovik DE, Aikawa E, Libby P, Weissleder R. Noninvasive vascular cell adhesion molecule-1 imaging identifies inflammatory activation of cells in atherosclerosis. Circulation 2006;114:1504–1511. [PubMed: 17000904]

25. Nahrendorf M, Sosnovik DE, Waterman P, Swirski FK, Pande AN, Aikawa E, Figueiredo JL, Pittet MJ, Weissleder R. Dual channel optical tomographic imaging of leukocyte recruitment and protease activity in the healing myocardial infarct. Circ Res 2007;100:1218–1225. [PubMed: 17379832]

26. Perez JM, Josephson L, O'Loughlin T, Hogemann D, Weissleder R. Magnetic relaxation switches capable of sensing molecular interactions. Nat Biotechnol 2002;20:816–820. [PubMed: 12134166]

27. Schellenberger EA, Sosnovik D, Weissleder R, Josephson L. Magneto/optical annexin V, a multimodal protein. Bioconjug Chem 2004;15:1062–1067. [PubMed: 15366960]

28. Shen T, Weissleder R, Papisov M, Bogdanov A Jr, Brady TJ. Monocrystalline iron oxide nanocompounds (MION): physicochemical properties. Magn Reson Med 1993;29:599–604. [PubMed: 8505895]

29. Simon GH, Bauer J, Saborovski O, Fu Y, Corot C, Wendland MF, Daldrup-Link HE. T1 and T2 relaxivity of intracellular and extracellular USPIO at 1.5T and 3T clinical MR scanning. Eur Radiol 2006;16:738–745. [PubMed: 16308692]

30. Sirol M, Itskovich VV, Mani V, Aguinaldo JG, Fallon JT, Misselwitz B, Weinmann HJ, Fuster V, Toussaint JF, Fayad ZA. Lipid-rich atherosclerotic plaques detected by gadofluorine-enhanced in vivo magnetic resonance imaging. Circulation 2004;109:2890–2896. [PubMed: 15184290]

31. Sosnovik DE, Nahrendorf M, Deliolanis N, Novikov M, Aikawa E, Josephson L, Rosenzweig A, Weissleder R, Ntziachristos V. Fluorescence tomography and magnetic resonance imaging of myocardial macrophage infiltration in infarcted myocardium in vivo. Circulation 2007;115:1384–1391. [PubMed: 17339546]

32. Sosnovik DE, Nahrendorf M, Weissleder R. Molecular magnetic resonance imaging in cardiovascular medicine. Circulation 2007;115:2076–2086. [PubMed: 17438163]

33. Sosnovik DE, Schellenberger EA, Nahrendorf M, Novikov MS, Matsui T, Dai G, Reynolds F, Grazette L, Rosenzweig A, Weissleder R, Josephson L. Magnetic resonance imaging of cardiomyocyte apoptosis with a novel magneto-optical nanoparticle. Magn Reson Med 2005;54:718–724. [PubMed: 16086367]

34. Stuber M, Gilson W, Schaer M, Bulte J, Kraitchman D. Shedding light on the dark spot with IRON—a method that generates positive contrast in the presence of superparamagnetic nanoparticles. Proc Intl Soc Magn Reson Med 2005;13:2608.

35. Sun EY, Josephson L, Kelly KA, Weissleder R. Development of nanoparticle libraries for biosensing. Bioconjug Chem 2006;17:109–113. [PubMed: 16417258]

36. Trivedi RAJMUK-I, Graves MJ, Cross JJ, Horsley J, Goddard MJ, Skepper JN, Quartey G, Warburton E, Joubert I, Wang L, Kirkpatrick PJ, Brown J, Gillard JH. In vivo detection of macrophages in human carotid atheroma: temporal dependence of ultrasmall superparamagnetic particles of iron oxide-enhanced MRI. Stroke 2004;35:1631–1635. [PubMed: 15166394]

37. van Tilborg GA, Mulder WJ, Chin PT, Storm G, Reutelingsperger CP, Nicolay K, Strijkers GJ. Annexin A5-conjugated quantum dots with a paramagnetic lipidic coating for the multimodal detection of apoptotic cells. Bioconjug Chem 2006;17:865–868. [PubMed: 16848390]

38. Vaughan T, DelaBarre L, Snyder C, Tian J, Akgun C, Shrivastava D, Liu W, Olson C, Adriany G, Strupp J, Andersen P, Gopinath A, van de Moortele PF, Garwood M, Ugurbil K. 9.4T human MRI: preliminary results. Magn Reson Med 2006;56:1274–1282. [PubMed: 17075852]

39. Wagner S, Schnorr J, Pilgrimm H, Hamm B, Taupitz M. Monomer-coated very small superparamagnetic iron oxide particles as contrast medium for magnetic resonance imaging: preclinical in vivo characterization. Invest Radiol 2002;37:167–177. [PubMed: 11923639]

40. Weissleder R, Kelly K, Sun EY, Shtatland T, Josephson L. Cell-specific targeting of nanoparticles by multivalent attachment of small molecules. Nat Biotechnol 2005;23:1418–1423. [PubMed: 16244656]

41. Weissleder R, Lee AS, Khaw BA, Shen T, Brady TJ. Antimyosin-labeled monocrystalline iron oxide allows detection of myocardial infarct: MR antibody imaging. Radiology 1992;182:381–385. [PubMed: 1732953]

42. Weissleder R, Stark DD, Engelstad BL, Bacon BR, Compton CC, White DL, Jacobs P, Lewis J. Superparamagnetic iron oxide: pharmacokinetics and toxicity. AJR Am J Roentgenol 1989;152:167–173. [PubMed: 2783272]

43. Winter PM, Morawski AM, Caruthers SD, Fuhrhop RW, Zhang H, Williams TA, Allen JS, Lacy EK, Robertson JD, Lanza GM, Wickline SA. Molecular imaging of angiogenesis in early-stage atherosclerosis with alpha(v)beta3-integrin-targeted nanoparticles. Circulation 2003;108:2270–2274. [PubMed: 14557370]

44. Winter PM, Neubauer AM, Caruthers SD, Harris TD, Robertson JD, Williams TA, Schmieder AH, Hu G, Allen JS, Lacy EK, Zhang H, Wickline SA, Lanza GM. Endothelial alpha(v)beta3 integrin-targeted fumagillin nanoparticles inhibit angiogenesis in atherosclerosis. Arterioscler Thromb Vasc Biol 2006;26:2103–2109. [PubMed: 16825592]

45. Wunderbaldinger P, Josephson L, Weissleder R. Crosslinked iron oxides (CLIO): a new platform for the development of targeted MR contrast agents. Acad Radiol 2002;9(Suppl 2):S304–306. [PubMed: 12188255]

46. Wunderbaldinger P, Josephson L, Weissleder R. Tat peptide directs enhanced clearance and hepatic permeability of magnetic nanoparticles. Bioconjug Chem 2002;13:264–268. [PubMed: 11906263]

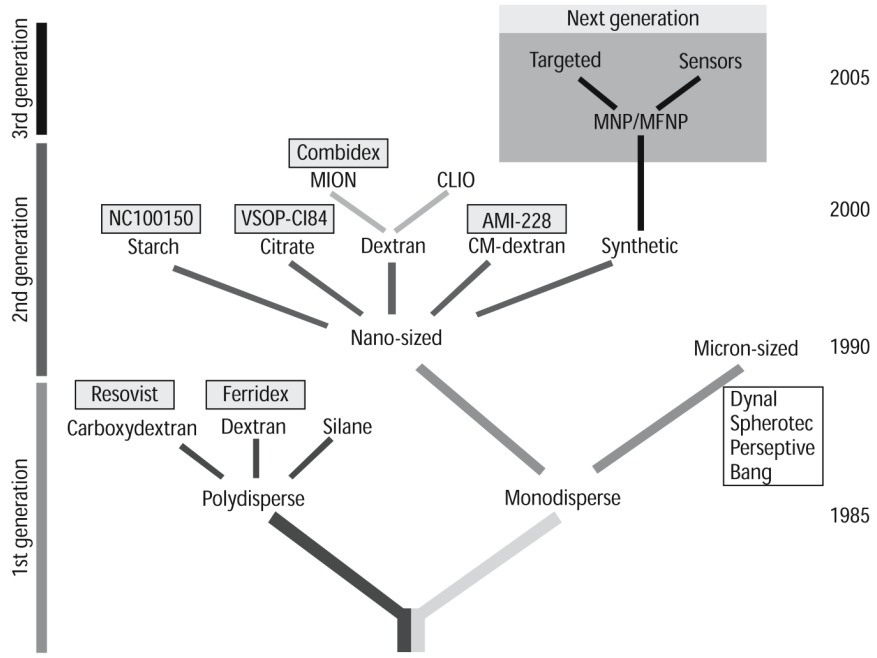

Fig. 1.

Schematic representation of advances in magnetic nanoparticle (MNP) design. MNP agents currently under development will have significantly higher relaxivities than earlier generations of MNP, and will also have improved synthetic coats for targeted imaging

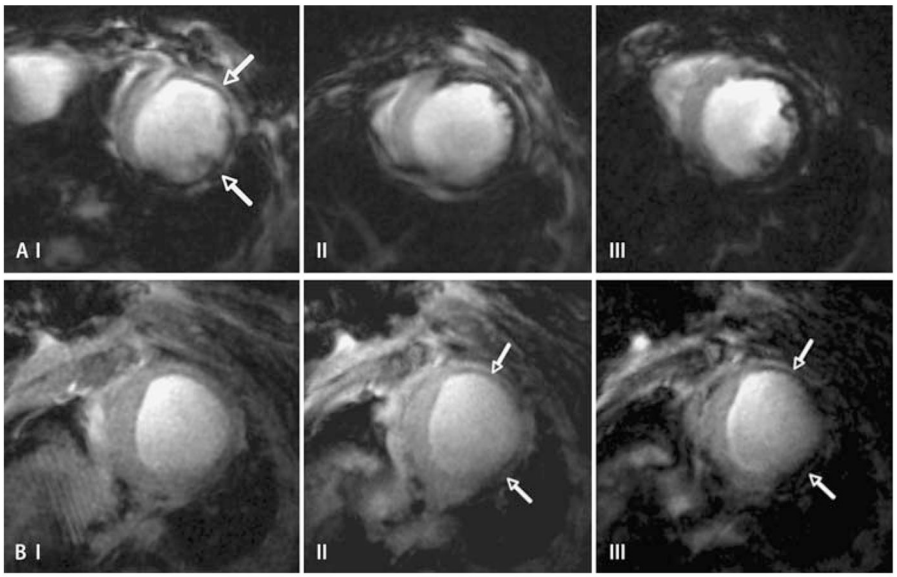

Fig. 2.

Panel **a**: conventional T2* weighted gradient echo imaging (echo time 6.5 ms) in three mice injected with CLIO-Cy5.5 48 h after infarction [31]. The injected doses were (*I*) 3 mg Fe/kg, (*II*) 10 mg Fe/kg and (*III*) 20 mg Fe/kg. Accumulation of the probe in macrophages produced signal hypointensity (negative contrast) in the injured anterolateral wall (*arrows*). A clear and fairly linear dose response was seen, even at doses significantly higher than those that could be given clinically. *Panel* **b**: conventional T2* weighted gradient echo imaging in a single mouse injected with 20 mg Fe/kg of CLIO-Cy5.5 48 h after infarction [31]. The images shown were obtained with an echo time of (*I*) 2.7 ms, (*II*) 3.5 ms and (*III*) 6.5 ms. The thinned infarcted anterolateral wall is clearly seen at the shortest echo time and develops negative contrast, due to MNP accumulation, only once the echo time is increased

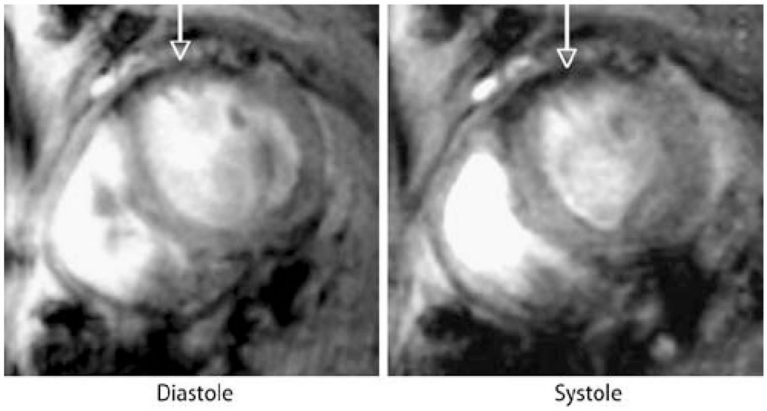

Fig. 3.

Imaging of cardiomyocyte apoptosis by MRI at 9.4 Tesla in mice in vivo [33]. The mice were injected with the annexin labeled MNP, AnxCLIO-Cy5.5, after transient coronary ligation. Accumulation of the probe was seen in the hypokinetic anterior wall of all mice injected with AnxCLIO-Cy5.5, as shown above (*arrows*). However, no accumulation of the unlabeled control probe, CLIO-Cy5.5, was seen in any of the mice

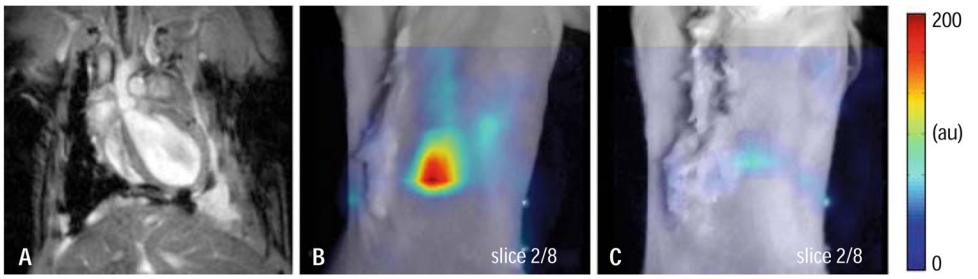

Fig. 4.

Dual modality imaging of the magnetofluorescent contrast agent, CLIO-Cy5.5 [31]. (see also Fig. 2 above). The images shown are: **a** coronal MR image of the thorax, through the plane of the heart, used for co-alignment with fluorescence tomography images of the heart and thorax. **b** 2D coronal slice at the level of the heart from a 3D fluorescence tomographic dataset. The fluorescence image has been overlaid onto a white light image of the mouse. The depth resolved 3D fluorescence dataset has been acquired completely non-invasively with a dedicated small animal fluorescence tomography system. Significant fluorescence signal is seen over the heart of an infarcted mouse, further confirming the presence of the MNP in the myocardium. **c** No significant fluorescence intensity is seen over the heart of a sham operated mouse

Table 1

Selected superparamagnetic iron oxide nanoparticles (MNP)

	Comment
Short circulating	
Ferumoxides (Feridex)	Approved liver imaging agent. Use for stem cell labeling is experimental
Ferrixan (Resovist)	Approved liver imaging agent
Long circulating	
Ferumoxtran (Combidex, AMI 227)	Completed phase 3 trials (lymph node imaging). Experience imaging plaque macrophages in humans is highly preliminary
Ferumoxytol (AMI 228)	Studied for iron replacement Rx
Monocrystalline iron oxide (MION-47)	Experimental nanoparticle highly similar to Ferumoxtran. Used extensively in animal models
Monocrystalline iron oxide (MION-48)	Experimental nanoparticle with extremely high transverse relaxivity (R2)
Cross linked iron oxide (CLIO)	Experimental nanoparticle, developed for targeted imaging
Very small superparamagnetic iron oxides (VSOP)	Citrate coated iron oxide nanoparticle

Table 2

Potential artifacts in cardiovascular molecular MRI

	Comment
Gadolinium constructs	
Incomplete fat suppression	May mimic probe uptake in the vascular wall (improve shim or use inversion recovery techniques)
Incomplete suppression of signal from blood pool due to slow flow	May compromise evaluation of probe uptake by atherosclerotic plaque (use of diffusion encoded stimulated echo techniques to improve signal loss in blood pool)
B1 inhomogeneity	Variable flip angle can produce inconsistent contrast in image. Problem only in humans and larger animals at higher field strengths (RF shimming with multiple transmit coils)
Ghosting from chest wall fat into region of interest	(use of breathold sequence and/or fat suppression)
Iron oxide nanoparticles	
Calcification	Low signal may mimic MNP uptake. (MION produces bright signal with T1 or positive contrast techniques)
Air	Low signal may mimic MNP uptake (MION produces bright signal with T1 or positive contrast techniques)
Susceptibility Artifacts	Can produce either non-specific negative or positive contrast depending on whether on-resonance or off-resonance imaging is performed (compare to conventional spin echo image)
Hemorrhage	Endogenous iron products may mimic exogenous MNP accumulation. Exceedingly rare in mouse heart. Incidence in humans will require study (dual modality imaging combining MRI with Fluorescence or PET would resolve issue)
Motion	Can dephase MR signal producing signal loss (reduce echo time, use gradient moment nulling, change to off-resonance technique with short echo time)

Potential solutions to these artifacts are shown in parenthesis